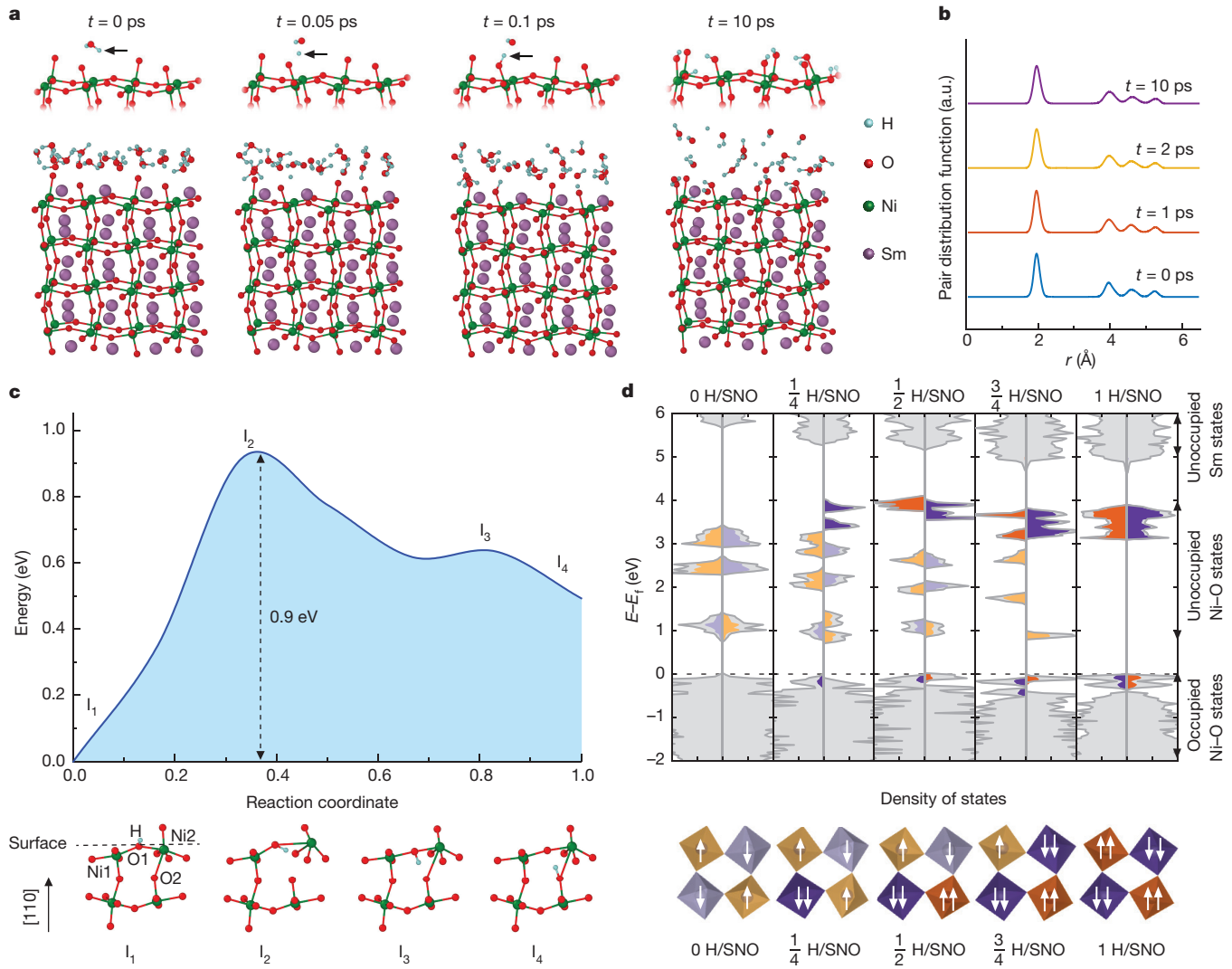


**Figure 3 | First-principles calculations of SNO–water interaction and HSNO. a**, AIMD simulations of water-mediated protonation of a SNO surface at 300 K. The top images show the evolution of a representative water molecule and the $NiO_6$ octahedra in the SNO layer closest to water. **b**, Surface stability of SNO, characterized by the Ni–O pair distribution function as a function of the separation distance *r* at various time intervals. **c**, Energy landscape and atomic-scale pathway of intercalation of surface protons into the SNO lattice. The potential energy is shown along the most preferred migration pathway, together with selected configurations along this pathway (labelled as $I_1$–$I_4$). **d**, First-principles calculation of hydrogen-intercalated SNO. The top panel shows the total density of states (grey) as a function of the difference between the energy (*E*) and the Fermi energy ($E_f$), with 0–1 added H atoms per SNO formula unit. The unoccupied projected density of states on each Ni site and the Ni projected density of states associated with localized electrons are shown in orange and purple, respectively, corresponding to inequivalent Ni sites. The lower panel shows a schematic of the occupied Ni $e_g$ levels for each scenario. The darker hues indicate Ni sites with two occupied $e_g$ states and the colours correspond to those in the upper panel.

aqueous environment is therefore $H^+_{aqueous} + SNO_{solid} + e^- \leftrightarrow HSNO_{solid}$, where the valence of Ni ions is reduced from Ni(III) in SNO to Ni(II) in HSNO.

*Ab initio* molecular dynamics (AIMD) simulations were carried out to study the underlying atomic-scale mechanisms of the water-mediated phase transition in SNO. As Fig. 3a shows, the water proximal to the SNO surface dissociates into a free proton and $OH^-$. The proton migrates to the oxide/water interface and binds to a surface oxygen atom (Supplementary Video 1). We find an increased uptake of protons by the surface oxygen atoms of SNO, which has little impact on the structural integrity of the oxide interface (Fig. 3a, $t = 10$ ps). The protonation of the SNO surface and its structural stability in water are also observed at elevated temperature (500 K; Extended Data Fig. 9a, b and Supplementary Video 2) and with either excess $OH^-$ radicals or excess protons. Besides primary surface events, such as proton migration and binding, the AIMD trajectories reveal that the $OH^-$ (arising from water dissociation) can bind to the under-coordinated Ni atoms (fewer than six O nearest neighbours) on the surface and restore the $NiO_6$ octahedra (Fig. 3a, $t = 10$ ps), which further improves the surface stability. The Ni–O pair distribution functions (Fig. 3b and Extended Data Fig. 9c) remain sharp and well defined. The peaks in the pair distribution functions can be resolved even at long distances (above 5 Å), indicating that the long-range structural order in SNO is preserved. The stability of the SNO surface stems in part from the high vacancy formation energies in pristine SNO; for example, the oxygen vacancy formation energy in SNO, as obtained from our density functional theory (DFT) calculations, is 2.95 eV, more than three times higher than the energy barrier for proton intercalation (0.9 eV in Fig. 3c).

Nudged elastic band calculations in the framework of DFT were performed to estimate the energy landscape and to identify the energetically preferred pathways for $H^+$ intercalation into SNO (Fig. 3c). Initially, the proton is bound to a surface oxygen atom O1 (image $I_1$ in Fig. 3c) at a distance of about 3.7 Å from atom O2, where atom O1 is the shared corner of two $NiO_6$ octahedra centred at nickel atoms Ni1


© 2017 Macmillan Publishers Limited, part of Springer Nature. All rights reserved.